HHS Public Access

Author manuscript

Kidney Int. Author manuscript; available in PMC 2012 October 01.

Published in final edited form as:

Kidney Int. 2012 April ; 81(7): 662–673. doi:10.1038/ki.2011.443.

Inhibition of glycogen synthase kinase 3β prevents NSAID-induced acute kidney injury

Hao Bao[1,2], **Yan Ge**[2], **Shougang Zhuang**[2], **Lance D Dworkin**[2], **Zhihong Liu**[1], and **Rujun Gong**[2]

[1]Research Institute of Nephrology, Jinling Hospital, Nanjing University School of Medicine, Nanjing, China

[2]Division of Kidney Disease and Hypertension, Brown University School of Medicine, Providence, Rhode Island, USA

Abstract

Clinical use of non-steroidal anti-inflammatory drugs (NSAIDs) like diclofenac (DCLF) is limited by multiple adverse effects, including renal toxicity leading to acute kidney injury. In mice with DCLF-induced nephrotoxicity TDZD-8, a selective glycogen synthase kinase (GSK)3β inhibitor, improved acute kidney dysfunction, ameliorated tubular necrosis and apoptosis associated with induced cortical expression of cyclooxygenase-2 (COX-2) and prostaglandin E2. This renoprotective effect was blunted but still largely preserved in COX-2 null mice, suggesting that other GSK3β targets beyond COX-2 functioned in renal protection. Indeed, TDZD-8 diminished the mitochondrial permeability transition in DCLF-injured kidneys. *In vitro*, GSK3β inhibition reinstated viability and suppressed necrosis and apoptosis in DCLF-stimulated tubular epithelial cells. DCLF elicited oxidative stress, enhanced the activity of the redox-sensitive GSK3β and promoted a mitochondrial permeability transition by interacting with cyclophilin D, a key component of the mitochondrial permeability transition pore. TDZD-8 blocked GSK3β activity, prevented GSK3β mediated cyclophilin D phosphorylation and the ensuing mitochondrial permeability transition, concomitant with normalization of intracellular ATP. Conversely, ectopic expression of a constitutively active GSK3β abolished the effects of TDZD-8. Hence, inhibition of GSK3β ameliorates NSAID-induced acute kidney injury by induction of renal cortical COX-2 and direct inhibition of the mitochondrial permeability transition.

Keywords

glycogen synthase kinase 3β; non-steroidal anti-inflammatory drugs; diclofenac; acute kidney injury; cyclooxygenase-2; mitochondrial permeability transition

Correspondence: Rujun Gong, MD, PhD, Division of Kidney Disease and Hypertension, Department of Medicine, Brown University School of Medicine, 593 Eddy Street, Providence, Rhode Island 02903, USA. Phone: +1 401-444-09899; Fax: +1 401-444-6849; Rujun_Gong@Brown.edu.

DISCLOSURE

All the authors declared no competing interests.

Introduction

Diclofenac (2-[(2,6-dichlorophenyl)amino]phenyl-acetate, DCLF) is one of the most frequently prescribed non-steroidal anti-inflammatory drugs (NSAIDs). Its clinical use is limited by the occurrence of DCLF-induced renal toxicity, which can manifest as acute kidney injury (AKI).[1, 2] Acute DCLF-induced nephrotoxicity involves both cyclooxygenase-dependent and -independent mechanisms. The blocking of cyclooxygenase (COX) and subsequent inhibition of prostaglandin (PG) synthesis by DCLF leads to renovascular constriction, renal ischemia, a decline in glomerular hydraulic pressure and AKI. Moreover, recent evidence suggests that mitochondria are a primary target of DCLF. [3-5] DCLF can directly induce the mitochondrial membrane permeability transition (MPT), which subsequently triggers cell death in multiple organs, including the kidney.[6-8]

Glycogen synthase kinase 3 β (GSK3β) is a ubiquitous serine-threonine protein kinase that participates in a multitude of cellular processes, including proliferation, apoptosis and necrosis, and plays an important role in the pathophysiology of a number of diseases, including kidney diseases. Previous studies have demonstrated that GSK3β inhibition induces COX-2 expression in the renal cortex.[9, 10] In addition, a growing body of evidence suggests that GSK3β inhibition plays a central role in both the ischemic and pharmacological preconditioning induced modulation of MPT induction.[11, 12] Inhibitory phosphorylation of GSK3β at serine 9 resulted in an elevated threshold for MPT activation and, consequently, protected from cell death.

In the present study, we examined the effects of 4-benzyl-2-methyl-1,2,4-thiadiazolidine-3,5-dione (TDZD-8), a novel, non-ATP competitive, highly selective small molecule inhibitor of GSK3β, on the development of DCLF-induced acute nephrotoxicity *in vivo* in a murine model of DCLF-induced nephrotoxicity and *in vitro* in cultured renal proximal tubular cells.

RESULTS

GSK3β inhibition improves general behavior and kidney function in DCLF-injured mice

Mice were pretreated with TDZD-8 or vehicle 1 h prior to injury by a nephrotoxic dose of DCLF (200 mg/kg) via oral gavages. Six hours later, illness and weakness became evident in the animals that received DCLF and vehicle alone. They were lethargic and reluctant to eat. Kidneys from DCLF-treated mice appeared enlarged and swollen, and markedly higher serum creatinine levels were detected in these mice, denoting acute kidney dysfunction (Table 1). In contrast, treatment with TDZD-8 significantly improved animal activity and food intake, attenuated weight loss and preserved renal function in DCLF-injured mice.

GSK3β inhibition prevents tubular necrosis and apoptosis in the kidneys of DCLF-injured mice

As shown in Figure 1, exposure to DCLF induced a typical pattern of acute tubular necrosis in the proximal and distal tubules, which was characterized by isometric vacuolization of the tubular epithelium, luminal ectasia, sloughing of tubular cells into the lumen, loss of brush border, nuclear enlargement and pleomorphism. To visualize apoptosis, TdT-mediated

dUTP nick-end labeling (TUNEL) staining was performed (Figure 1B, D, F, H, J). Scattered, bright TUNEL positive nuclei could be evidently observed over the entire cortex of the DCLF-injured kidneys but were rarely observed in the specimens from control mice. Both tubular necrosis and apoptosis were significantly attenuated in TDZD-8-treated mice.

TDZD-8 inhibits GSK3β activity and induces cortical COX-2 in DCLF-injured kidneys

In DCLF-injured kidneys, enhanced GSK3β activity was demonstrated by reduced inhibitory phosphorylation of GSK3β at serine 9. TDZD-8, a highly selective small molecule inhibitor of GSK3β, induced prominent phosphorylation of GSK3β in both control and DCLF-injured kidneys, denoting the inhibition of GSK3β kinase activity (Figure 2A). One important mechanism of NSAID-induced kidney injury is the inhibition of COX activity in the kidney. Indeed, PGE_2 levels in the renal cortices were significantly decreased in DCLF-injured kidneys (Figure 2C). The compensatory induction of renal cortical COX-2 was observed in DCLF-injured mice, and this was augmented following TDZD-8 treatment (Figure 2B). This is consistent with previous reports in other animal models that GSK3β inhibition induces COX-2 expression.[9, 10] The decreased PGE_2 levels in the renal cortex were partially abrogated after TDZD-8 treatment (Figure 2C).

Renal protective effects of GSK3β inhibition on DCLF-induced AKI is largely preserved in COX-2 null mice

To determine whether the beneficial effects of GSK3β inhibition were entirely mediated by the induction of COX-2 expression, COX-2 knockout mice were administered a nephrotoxic dose of DCLF following pretreatment with either TDZD-8 or vehicle. Shown in Figure 3, the renoprotective efficacy of TDZD-8 was slightly but significantly blunted in the COX-2 null mice, as evidenced by the difference in the tubular injury scores as well as in the serum creatinine levels (Figure 3B, Figure 3C) between the wild type and the knockout mice injured with DCLF and treated with TDZD-8, suggesting that COX-2 is involved in the mechanism of kidney protection. However, TDZD-8 could still effectively ameliorate the DCLF induced AKI and acute tubular necrosis in COX-2 null mice, and the renoprotective effect of TDZD-8 was actually largely preserved in COX-2 null mice, indicating that a COX-2/PGE_2 independent pathway also contributes, at least in part, to kidney protection.

GSK3β inhibition suppresses MPT in DCLF-injured kidneys

Both persistent ischemia and direct DCLF toxicity can induce MPT, a critical mechanism causing cell death. Whether TDZD-8 protects kidneys from DCLF induced MPT was studied next. In isolated mitochondria, the capacity to tolerate a calcium challenge is inversely correlated with the susceptibility to the MPT. To assess the MPT *in vivo*, renal mitochondria were purified, and calcium-induced mitochondrial swelling was measured as a decrease in spectrophotometric absorbance at 540 nm. As can be seen in Figure 4, mitochondria isolated from the kidneys of DCLF-treated mice displayed a greater decrease in absorbance at 540 nm upon calcium overload, denoting an accelerated rate of mitochondrial swelling and marked mitochondrial dysfunction. TDZD-8 treatment significantly ameliorated this effect in a dose dependent fashion (Figure 4). More importantly, the extent of calcium-induced mitochondrial swelling was negatively correlated

with both the number of apoptotic cells in the kidneys and the severity of renal histologic injury. These findings suggest that TDZD-8 protected renal cells from apoptosis and necrosis primarily by inhibiting MPT *in vivo*.

GSK3β inhibition improves the cell viability of renal tubular epithelial cells exposed to DCLF

To determine whether treatment with TDZD-8 ameliorated DCLF-induced AKI via a direct protective effect on renal tubular cells, cultured murine tubular epithelial (TKPT) cells were exposed to DCLF at different doses for different intervals in the presence or absence of TDZD-8. DCLF stimulation reduced cellular viability in a dose- (Figure 5A) and time- (Figure 5B) dependent manner, as assessed by tetrazolium (MTT) assays, and this effect could be significantly counteracted by treatment with TDZD-8 (Figure 5C). In contrast, in cells expressing S9A-GSK3β, an uninhibitable mutant of GSK3β in which serine 9 was replaced by alanine, the protective activity of TDZD-8 was blunted (Figure 5D), suggesting that the inhibitory phosphorylation of GSK3β is required for the protective effect of TDZD-8.

GSK3β inhibition protects from DCLF-induced apoptosis and necrosis in renal tubular epithelial cells

Shown in Figure 6, DCLF induced significant cell apoptosis within 24 h. Treatment with TDZD-8 significantly decreased the number of apoptotic cells, as detected by TUNEL staining, and the anti-apoptotic effect of TDZD-8 was attenuated in cells expressing S9A-GSK3β, indicating the indispensable role of phosphorylation in the inhibition of GSK3β. To assess necrosis, we undertook both a morphological examination of propidium iodide (PI) staining of cultured cells (Figure 7A, B) and a biochemical assay for the enzymatic activity of cytoplasmic lactate dehydrogenase (LDH) (Figure 7C), which is released into conditioned media upon cellular necrosis and rupture of the plasma membrane. DCLF stimulation augmented both LDH activity and PI positivity, and this was substantially reduced by treatment with TDZD-8. In cells expressing the S9A-GSK3β mutant, the anti-necrotic effect of TDZD-8 was likewise blunted, suggesting that inhibitory phosphorylation of GSK3β is essential for the protection of the cell by TDZD-8.

GSK3β inhibition attenuates DCLF-induced MPT in renal tubular epithelial cells

The mitochondrial dye tetramethylrhodamine methyl ester (TMRM) was used to monitor the onset of the MPT in cultured TKPT cells. Under basal conditions, the lipophilic TMRM, which bears a delocalized positive charge, enters the negatively charged mitochondria and accumulates in a potential-dependent manner along the inner membrane (Figure 8A). Upon MPT, the mitochondrial membrane permeability transition pore opens, and the TMRM potentiometric dye no longer accumulates inside the mitochondria but is instead distributed throughout the cytosol. In our study, following DCLF stimulation, the overall cellular fluorescence intensity dropped dramatically (Figure 8A), denoting the onset of the MPT. TDZD-8 successfully counteracted the DCLF-elicited quenching of TMRM, and this effect was similarly blunted in cells expressing the mutant S9A-GSK3β (Figure 8A).

Calcium overload-induced mitochondrial swelling, as measured by a decrease in spectrophotometric absorbance at 540 nm, was similarly employed to detect the MPT (Figure 8B, C). There was a negative correlation between the reduction in absorbance at 540 nm and the number of apoptotic or necrotic cells (Figure 8C). Mitochondria that were isolated from cells treated with DCLF displayed increased swelling, while treatment with TDZD-8 attenuated this effect, which was likewise diminished in the mitochondria of cells expressing S9A-GSK3β (Figure 8B). All of these observations imply that the inhibition of GSK3β protects tubular cells from apoptosis and necrosis by inhibiting MPT pore opening *in vitro*.

GSK3β inhibition prevents DCLF-induced ATP reduction in renal tubular epithelial cells

MPT pore opening allows the reentry of protons, thus bypassing ATP synthase and preventing the generation of ATP by the mitochondria. Consistent with induction of the MPT, intracellular ATP levels were drastically diminished in DCLF-treated TKPT cells (Figure 9). Treatment with TDZD-8 retained intracellular ATP levels, while this effect was not apparent in cells expressing S9A-GSK3β, implying that the inhibition of GSK3β protects tubular cells from death by preserving intracellular ATP *in vitro*.

DCLF enhances the activity of redox-sensitive GSK3β in TKPT cells

Upon exposure to DCLF, the production of reactive oxygen species (ROS) was significantly increased, concomitant with increased GSK3β kinase activity and diminished inhibitory phosphorylation of GSK3β (Figure 10A, C, D), consistent with previous findings that GSK3β is a redox-sensitive kinase.[13] Mitochondria are a major source of ROS production, and two main sites of O_2^- and H_2O_2 generation in the inner mitochondrial membrane have been identified: complex I and complex III. To identify the source of ROS production in response to DCLF stimulation, rotenone and stigmatellin, inhibitors respectively for respiratory complexes I and III, were applied. Treatment with rotenone did not prevent the increase of ROS production or enhanced GSK3β activity, denoting that complex I is not the main site of DCLF increased ROS production. Consistently, DCLF failed to produce a direct effect on the activity of NADH dehydrogenase (Figure 10B). In contrast, treatment with stigmatellin significantly suppressed the production of ROS and the activation of GSK3β (Figure 10A, C, D), suggesting that mitochondrial ROS formation, particularly at respiratory chain complex III, is involved in DCLF enhanced activity of redox-sensitive GSK3β.

GSK3β inhibition prevents cyclophilin D phosphorylation in the mitochondria of TKPT cells exposed to DCLF

To explore whether and how GSK3β directly regulates MPT, the expression of GSK3β in the mitochondria of TKPT cells was examined. Fluorescent immunocytochemistry indicated that a significant amount of GSK3β staining co-localized with mitochondrial staining, in agreement with the specific, subcellular distribution of GSK3β in the mitochondria (Figure 11A). To corroborate the morphological findings, immunoprecipitation was performed and revealed that GSK3β co-precipitated with cyclophilin D (Figure 11B), indicating that GSK3β physically interacts with cyclophilin D, a component of the MPT pore complex.

To further explore the mechanism by which GSK3β regulates cyclophilin D activation, the cyclophilin D amino acid sequence was analyzed. Residues Ser118 and Ser190 of mitochondrial cyclophilin D reside in consensus motifs (SXXXS) for phosphorylation by GSK3β. Shown in Figure 11C, DCLF treatment significantly increased the phosphorylation of cyclophilin D. Conversely, inhibition of GSK3β by TDZD-8 suppressed the phosphorylation of cyclophilin D, whereas this effect was diminished in cells transfected with S9A-GSK3β. Together, these results suggest that GSK3β inhibition stabilizes the MPT by suppressing cyclophilin D phosphorylation in the mitochondria of TKPT cells exposed to DCLF.

DISCUSSION

NSAIDs are prescribed to millions worldwide for the treatment of osteoarthritis, rheumatoid arthritis, and muscle pain.[14] In 2008 alone, over 107,000 NSAIDs-related toxicity cases were reported, more than 14,000 cases of which required treatment in health care facilities. DCLF is one of the most frequently prescribed NSAIDs. A literature search on DCLF-induced renal toxicity in humans identified a number of cases, most associated with acute renal failure and some of which were fatal.[1, 2]

Basal prostaglandins maintain normal glomerular perfusion and glomerular filtration rate. The inhibition of prostaglandin synthesis by DCLF leads to renal ischemia, a decline in glomerular hydraulic pressure and acute renal failure. GSK3β, a constitutively active protein kinase with an important regulatory role in cell signaling, differentiation, gene expression and apoptosis, has been implicated in the pathogenesis of multiple kidney diseases, both chronic and acute.[15-19] In the present study, we found that the inhibition of GSK3β activity by TDZD-8, a small molecule inhibitor of GSK3β, ameliorated DCLF-induced AKI. This was associated with suppressed GSK3β activity, induced inhibitory phosphorylation of GSK3β, and increased COX-2 expression in the renal cortex. Consistently, PGE_2 concentrations in the renal cortex were significantly elevated. Our finding is in agreement with previous reports indicating that GSK3β inhibition may induce COX-2 expression via the negative regulation of extracellular signal-regulated kinases.[20] Of note, the renal protective effect of GSK3β inhibition by TDZD-8 was blunted but still largely preserved in COX-2 null mice, suggesting that GSK3β inhibition may attenuate renal injury through mechanisms that are beyond COX-2 induction.

In addition to the induction of acute ischemic kidney injury through the disturbance of prostaglandin homeostasis in the kidney, treatment with DCLF can impinge on renal tubular epithelial cells directly. Significantly, tubular cell mitochondria are a prime target of DCLF.[4] We found that mitochondria treated with DCLF were more likely to undergo mitochondrial swelling induced by calcium and were more susceptible to the shift of TMRM through the opened pores. MPT, an increase in the permeability of the mitochondrial membrane, is a common pathway leading to cell death. DCLF-induced apoptosis and necrosis were detected *in vivo* and *in vitro*, consistent with previous reports.[8, 21] 4′OH-DCLF and 5OH-DCLF are the major urine metabolites of DCLF in rodents and humans.[22] DCLF, 4′OH-DCLF and 5OH-DCLF induce concentration-dependent apoptosis, and at equimolar concentrations, the greatest pro-apoptotic activity was produced by 5OH-DCLF. [7]

The MPT is under orchestrated regulation by a myriad of cell signaling transducers, including GSK3β. Recent studies have demonstrated that GSK3β inhibition plays a central role in the transduction of protective signals by raising the MPT induction threshold.[11, 12, 23] The phosphorylation of GSK3β at serine 9 raised the MPT threshold and protected cells by inhibiting the signaling cascades associated with the induction of the MPT.[24, 25] In the present study, the inhibition of GSK3β activity by TDZD-8 successfully prevented the swelling of mitochondria that were isolated from DCLF-injured cells and tissues, and this effect was attenuated in mitochondria from cells expressing mutant GSK3β that is not able to be inhibited via phosphorylation at serine 9, demonstrating that GSK3β inhibition diminishes DCLF-triggered MPT pore opening. Our findings are in agreement with a previous study by Plotnikov et al. in which treatment with lithium ion, an inhibitor of GSK3β, restored the mitochondrial membrane potential in tubular cells from rat kidneys that were subjected to ischemic reperfusion.[26] In the present study, in murine TKPT cells, DCLF induced a strong ROS burst and oxidative stress. Although ROS can cause cell destruction by massive lipid peroxidation, in most cases, ROS modulates signal transduction pathways by affecting oxidation-reduction (redox)-sensitive enzymes, organelles, and signaling transducers, such as GSK3β. Indeed, the DCLF-elicited ROS burst was associated with the enhanced activation of GSK3β, and both were abrogated by treatment with stigmatellin but not rotenone. This suggests that DCLF can interfere with the mitochondrial electron transport chain, leading to augmented activation of the redox-sensitive GSK3β kinase. Moreover, a significant subcellular distribution of GSK3β was found to be co-localized with the mitochondria, suggesting a potential regulatory role for GSK3β in mitochondrial function. Thus far, the only MPT components to be identified are the peripheral benzodiazepine receptor, located in the mitochondrial outer membrane, and cyclophilin D, localized to the matrix.[27, 28] Residues Ser118 and Ser190 of mitochondrial cyclophilin D reside in GSK3β phosphorylation consensus motifs. DCLF treatment significantly increased the phosphorylation of cyclophilin D, which may trigger the opening of the end-effector MPT pore. Permeability of the mitochondrial inner membrane allow solutes with a molecular weight of less than 1500 to leak from the mitochondria, and the subsequent breaking of mitochondrial outer membrane leads to the release of proteins and cell death.[28, 29] Conversely, inhibition of GSK3β successfully prevented the phosphorylation of cyclophilin D in the mitochondria, which may leads to the stabilization of the MPT.

Mitochondria play a crucial role in maintaining ATP-dependent cellular processes.[30] MPT pore opening allows the massive reentry of protons into the mitochondrial matrix, thus bypassing ATP synthase and preventing ATP synthesis.[31] In this study, we observed a significant reduction in ATP levels in DCLF injured cells, consistent with the findings of both Mingatto et al.[5] and Ng et al.[32], that DCLF depressed the rate of ATP synthesis. The progression to necrotic or apoptotic cell death depends, in part, on the effect of the opening of the MPT pore on cellular ATP levels.[33] If many pores open, the major drop in cellular ATP levels triggers cellular swelling and rupture of the plasma membrane, and thus, necrotic cell death ensues; if ATP levels are at least partially maintained, the MPT is followed by apoptosis. GSK3β inhibition has been shown to be a successful therapeutic strategy to prevent hepatic mitochondrial dysfunction and improve the preservation of cellular ATP content following ischemic reperfusion injury.[34] In this study, we observed that, following

the inhibition of GSK3β by TDZD-8, DCLF-elicited MPT was suppressed, and intracellular ATP levels were restored, leading to reduced tubular cell death.

In conclusion, TDZD-8, a highly selective inhibitor of GSK3β, attenuates DCLF-induced AKI, suppresses tubular cell death, and improves kidney function by inducing renal cortical COX-2 expression and inhibiting MPT in a DCLF-induced nephrotoxicity model (Figure 12). Our findings suggest that the inhibition of GSK3β by either novel selective small molecule inhibitors or existing FDA approved drugs with GSK3β inhibitory activity, such as lithium and valproate, represents a novel therapeutic strategy for AKI, particularly for NSAID-induced AKI.

METHODS

Animal experimental design

Animal experimental studies were approved by the institution's Animal Care and Use Committee and they conform to the USDA regulations and the NIH guidelines for humane care and use of laboratory animals. Drugs were given as previously described. [8, 35] BALB/c mice aged 6-8 weeks were randomly assigned to one of the five groups, and sacrificed 24 h after DCLF administration.

Group C (*n* =6), control mice received vehicle alone;

Group T (*n*=6), mice were only treated with selective GSK3β inhibitor TDZD-8 (5 mg/kg, i.v. dissolved in 10% DMSO);

Group D (*n*=6), mice were subjected to DCLF (200 mg/kg) injury by oral gavage and vehicle was given 1 hour before DCLF injury;

Group T-L+D (*n*=6), mice were subjected to DCLF (200 mg/kg) injury by oral gavage. Low dose TDZD-8 (1mg/Kg, i.v. dissolved in 10% DMSO) was given 1 hour before DCLF injury;

Group T+D (*n* =6), mice were subjected to DCLF (200 mg/kg) injury by oral gavage. TDZD-8 (5mg/Kg, i.v. dissolved in 10% DMSO) was given 1 hour before DCLF injury.

Congenic COX-2 knockout mice on a BALB/c background were bred by backcrossing the COX-2 knockout mice on a mixed 129/C57 background, which were originally obtained from the Jackson Laboratory (Bar Harbor, ME, USA), with the inbred BALB/c mice for more than 10 generations. Congenic homozygous COX-2 null mice were bred by brother/sister mating of heterozygous animals of the tenth generation. Genotyping was performed as previously described.[36]

Renal pathology

Kidney sections were prepared and stained as previously described.[37] Acute tubular injury was accessed using semi-quantitative measurements according to the proportion relative to the total section area and classified as follows: 0 (nil), 1 (<25%), 2 (25–50%), 3 (50–75%), and 4 (>75% of tubules).

Western immunoblot analysis and immunoprecipitation

Western immunoblot was performed as previously described.[15] The antibodies against GSK3β, p-GSK3β, COX-1 and COX-2 were purchased from Santa Cruz Biotechnology (Santa Cruz, CA, USA). For detection of phosphorylated cyclophilin D, cyclophilin D antibody (Santa Cruz Biotechnology) was used as the immunoprecipitation (IP) antibody and the antibody against phosphorylated serine (Santa Cruz Biotechnology) was used to probe the IP products by immunoblot analysis.

Measurement of PGE_2 in kidney cortex

The PGE_2 was measured by an enzymatic immunoassay kit from Cayman Chemical (Ann Arbor, MI, USA) according to the manufacturer's instruction.

Reverse transcription PCR

Reverse transcription PCR (RT-PCR) was performed as previously described using specific primers (*COX-2* sense, 5′-GTGGAAAAACCTCGTCCAGA-3′, *COX-2* antisense, 5′-TGATGGTGGCTGTTTTGGTA-3′).[38]

Cell culture and plasmid transfection

Murine proximal tubule epithelial (TKPT) cells were grown in DMEM/F12 that contained 5% fetal bovine serum. The eukaryotic expression vectors encoding uninhibitable mutant (S9A-GSK3β-HA/pcDNA3) were provided by Dr. Johnson (Birmingham, AL), [39] and were transfected as previously described. [15] Immunofluorescent staining revealed that more than 75% of the cells expressed the hemagglutinin-tagged constructs 24h after transfection. Cells were then subjected to different treatments, and assessed by MTT viability assay.[40]

Measurement of cell apoptosis

TUNEL staining was performed on fixed tissue sections or cell cultures with a cell apoptosis detection kit (Roche Applied Science, Indianapolis, IN, USA) according to the manufacturer's instructions.

Measurement of cell necrosis

Necrotic cell death was assessed by the PI exclusion assay and LDH release in the medium as previously described.[41]

Mitochondrial permeability transition assay

Mitochondria were isolated from kidney cells as previously described.[4, 42] The protein concentration was determined with BSA as the standard. Mitochondrial swelling was estimated based on the decrease in the absorbance of mitochondria (1.0 mg protein) at 540 nm in 1 ml of a medium containing 125 mM sucrose, 65 mM KCl, 5 mM succinate, 5 M rotenone, 20 M $CaCl_2$ and 10 mM Hepes-KOH, pH 7.2, at 30°C.

Fluorescent analysis of mitochondrial permeability transition

MPT pore opening in cultured cells was assessed using Tetramethylrhodamine methyl ester (TMRM, Sigma). In brief, after different treatments, TMRM (100nM) was added to culture

and incubated at 37 °C for 15 min.[43] Results were interpreted using a fluorescence microscopy.

ATP assay

ATP content in cells was measured by the luciferase method in freshly prepared cellular lysates using the ATP bioluminescence assay kit provided by Roche Applied Science according to the manufacturer's instructions.

Measurement of NADH dehydrogenase activity

The rotenone-sensitive reduction of decylubiquinone was measured following the procedure reported for respiratory complex I activity using a freeze-thawed mitochondrial extract (containing 0.3 mg protein).[32] NADH fluorescence intensity was monitored at Ex/Em of 352/464 nm in the absence or presence of 200μM DCLF or 1μM rotenone which served as a positive control.

ROS production assay

ROS production in isolated cells was measured using 2′,7′-Dichlorodihydrofluorescein diacetate (DCFH-DA) as previously described.[44]

GSK3β kinase activity assay

GSK3β kinase activity was determined using an assay kit commercially available from the Sigma according to the manufacturer's instructions.

Fluorescent immunocytochemistry

TKPT cells were stained with MitoTracker Green FM (150nM, Molecular Probes, Carlsbad, CA, USA) for 20 min, and then fixed with 4% paraformaldehyde and counterstained with anti-GSK3β antibodies as previously described. [45]

Statistical analyses

For immunoblot analysis, bands were scanned and the integrated pixel density was determined using a densitometer and an NIH image analysis program. All data are expressed as mean±SD. Statistical analysis of the data from multiple groups was performed by one-way ANOVA followed by Student-Newman-Kuels test. Data from two groups were compared by t test. $P< 0.05$ was considered significant.

ACKNOWLEDGEMENTS

Dr. Hao Bao is an International Society of Nephrology (ISN) Fellow and a recipient of the ISN fellowship. This work was made possible by the funding from the National Basic Research Program of China 973 Program No. 2012CB517600, the ISN Sister Renal Center Program, the Developmental Grant from Brown Medical School Department of Medicine and the National Institutes of Health Grant R01DK092485. We are indebted to Drs. Rifai and Yang for stimulating discussions and helpful suggestions.

REFERENCES

1. Rubio GJA, Tellez MMJ. Acute renal failure and nephrotic syndrome associated with treatment with diclofenac. Rev Clin Esp. 1992; 191:289–290.

2. Cicuttini L, Colatutto A, Pellegrini MA, et al. Acute reversible renal insufficiency during treatment with diclofenac. Clin Ter. 1989; 128:81–86. [PubMed: 2523777]
3. Masubuchi Y, Nakayama S, Horie T. Role of mitochondrial permeability transition in diclofenac-induced hepatocyte injury in rats. Hepatology. 2002; 35:544–551. [PubMed: 11870366]
4. Uyemura SA, Santos AC, Mingatto FE, et al. Diclofenac sodium and mefenamic acid: potent inducers of the membrane permeability transition in renal cortex mitochondria. Arch Biochem Biophys. 1997; 342:231–235. [PubMed: 9186483]
5. Mingatto FE, Santos AC, Uyemura SA, et al. In vitro interaction of nonsteroidal anti-inflammatory drugs on oxidative phosphorylation of rat kidney mitochondria: respiration and ATP synthesis. Arch Biochem Biophys. 1996; 334:303–308. [PubMed: 8900405]
6. Gomez-Lechon MJ, Ponsoda X, O'Connor E, et al. Diclofenac induces apoptosis in hepatocytes. Toxicol In Vitro. 2003; 17:675–680. [PubMed: 14599462]
7. Gomez-Lechon MJ, Ponsoda X, O'Connor E, et al. Diclofenac induces apoptosis in hepatocytes by alteration of mitochondrial function and generation of ROS. Biochem Pharmacol. 2003; 66:2155–2167. [PubMed: 14609740]
8. Hickey EJ, Raje RR, Reid VE, et al. Diclofenac induced in vivo nephrotoxicity may involve oxidative stress-mediated massive genomic DNA fragmentation and apoptotic cell death. Free Radic Biol Med. 2001; 31:139–152. [PubMed: 11440826]
9. Kotnik P, Nielsen J, Kwon TH, et al. Altered expression of COX-1, COX-2, and mPGES in rats with nephrogenic and central diabetes insipidus. Am J Physiol Renal Physiol. 2005; 288:F1053–1068. [PubMed: 15644490]
10. Kwon T. Dysregulation of Renal Cyclooxygenase-2 in Rats with Lithium-induced Nephrogenic Diabetes Insipidus. Electrolyte & Blood Pressure. 2007:68–74. [PubMed: 24459504]
11. Juhaszova M, Zorov DB, Kim SH, et al. Glycogen synthase kinase-3beta mediates convergence of protection signaling to inhibit the mitochondrial permeability transition pore. J Clin Invest. 2004; 113:1535–1549. [PubMed: 15173880]
12. Xi J, Wang H, Mueller RA, et al. Mechanism for resveratrol-induced cardioprotection against reperfusion injury involves glycogen synthase kinase 3beta and mitochondrial permeability transition pore. Eur J Pharmacol. 2009; 604:111–116. [PubMed: 19135050]
13. Wang SH, Shih YL, Kuo TC, et al. Cadmium toxicity toward autophagy through ROS-activated GSK-3beta in mesangial cells. Toxicol Sci. 2009; 108:124–131. [PubMed: 19126599]
14. Murray MD, Brater DC. Renal toxicity of the nonsteroidal anti-inflammatory drugs. Annu Rev Pharmacol Toxicol. 1993; 33:435–465. [PubMed: 8494347]
15. Gong R, Rifai A, Ge Y, et al. Hepatocyte growth factor suppresses proinflammatory NFkappaB activation through GSK3beta inactivation in renal tubular epithelial cells. J Biol Chem. 2008; 283:7401–7410. [PubMed: 18201972]
16. Gong R, Rifai A, Dworkin LD. Activation of PI3K-Akt-GSK3beta pathway mediates hepatocyte growth factor inhibition of RANTES expression in renal tubular epithelial cells. Biochem Biophys Res Commun. 2005; 330:27–33. [PubMed: 15781227]
17. Nelson PJ, Cantley L. GSK3beta plays dirty in acute kidney injury. J Am Soc Nephrol. 2010; 21:199–200. [PubMed: 20056749]
18. Ge Y, Si J, Tian L, et al. Conditional ablation of glycogen synthase kinase 3beta in postnatal mouse kidney. Lab Invest. 2011; 91:85–96. [PubMed: 20680007]
19. Wang Z, Havasi A, Gall J, et al. GSK3beta promotes apoptosis after renal ischemic injury. J Am Soc Nephrol. 2010; 21:284–294. [PubMed: 20093356]
20. Wang Q, Zhou Y, Wang X, et al. Glycogen synthase kinase-3 is a negative regulator of extracellular signal-regulated kinase. Oncogene. 2006; 25:43–50. [PubMed: 16278684]
21. Ng LE, Halliwell B, Wong KP. Nephrotoxic cell death by diclofenac and meloxicam. Biochem Biophys Res Commun. 2008; 369:873–877. [PubMed: 18325323]
22. Stierlin H, Faigle JW. Biotransformation of diclofenac sodium (Voltaren) in animals and in man. II. Quantitative determination of the unchanged drug and principal phenolic metabolites, in urine and bile. Xenobiotica. 1979; 9:611–621. [PubMed: 119353]
23. Zhai P, Sadoshima J. Overcoming an energy crisis?: an adaptive role of glycogen synthase kinase-3 inhibition in ischemia/reperfusion. Circ Res. 2008; 103:910–913. [PubMed: 18948628]

24. Yao LL, Huang XW, Wang YG, et al. Hydrogen sulfide protects cardiomyocytes from hypoxia/reoxygenation-induced apoptosis by preventing GSK-3beta-dependent opening of mPTP. Am J Physiol Heart Circ Physiol. 2010; 298:H1310–1319. [PubMed: 20154265]
25. Zorov DB, Juhaszova M, Yaniv Y, et al. Regulation and pharmacology of the mitochondrial permeability transition pore. Cardiovasc Res. 2009; 83:213–225. [PubMed: 19447775]
26. Plotnikov EY, Kazachenko AV, Vyssokikh MY, et al. The role of mitochondria in oxidative and nitrosative stress during ischemia/reperfusion in the rat kidney. Kidney Int. 2007; 72:1493–1502. [PubMed: 17914353]
27. Sileikyte J, Petronilli V, Zulian A, et al. Regulation of the inner membrane mitochondrial permeability transition by the outer membrane translocator protein (peripheral benzodiazepine receptor). J Biol Chem. 2011; 286:1046–1053. [PubMed: 21062740]
28. Baines CP, Kaiser RA, Purcell NH, et al. Loss of cyclophilin D reveals a critical role for mitochondrial permeability transition in cell death. Nature. 2005; 434:658–662. [PubMed: 15800627]
29. Green DR, Reed JC. Mitochondria and apoptosis. Science. 1998; 281:1309–1312. [PubMed: 9721092]
30. Bereiter-Hahn J, Jendrach M. Mitochondrial dynamics. Int Rev Cell Mol Biol. 2010; 284:1–65. [PubMed: 20875628]
31. Pessayre D, Mansouri A, Berson A, et al. Mitochondrial involvement in drug-induced liver injury. Handb Exp Pharmacol. 2010:311–365. [PubMed: 20020267]
32. Ng LE, Vincent AS, Halliwell B, et al. Action of diclofenac on kidney mitochondria and cells. Biochem Biophys Res Commun. 2006; 348:494–500. [PubMed: 16890207]
33. Lemasters JJ, Qian T, Bradham CA, et al. Mitochondrial dysfunction in the pathogenesis of necrotic and apoptotic cell death. J Bioenerg Biomembr. 1999; 31:305–319. [PubMed: 10665521]
34. Varela AT, Simoes AM, Teodoro JS, et al. Indirubin-3′-oxime prevents hepatic I/R damage by inhibiting GSK-3beta and mitochondrial permeability transition. Mitochondrion. 2010; 10:456–463. [PubMed: 20433952]
35. Dugo L, Abdelrahman M, Murch O, et al. Glycogen synthase kinase-3beta inhibitors protect against the organ injury and dysfunction caused by hemorrhage and resuscitation. Shock. 2006; 25:485–491. [PubMed: 16680013]
36. Alam I, Warden SJ, Robling AG, et al. Mechanotransduction in bone does not require a functional cyclooxygenase-2 (COX-2) gene. J Bone Miner Res. 2005; 20:438–446. [PubMed: 15746988]
37. Gong R, Rifai A, Tolbert EM, et al. Hepatocyte growth factor ameliorates renal interstitial inflammation in rat remnant kidney by modulating tubular expression of macrophage chemoattractant protein-1 and RANTES. J Am Soc Nephrol. 2004; 15:2868–2881. [PubMed: 15504940]
38. Ma X, Yang Q, Wilson KT, et al. Promoter methylation regulates cyclooxygenase expression in breast cancer. Breast Cancer Res. 2004; 6:R316–321. [PubMed: 15217498]
39. Cho JH, Johnson GV. Primed phosphorylation of tau at Thr231 by glycogen synthase kinase 3beta (GSK3beta) plays a critical role in regulating tau's ability to bind and stabilize microtubules. J Neurochem. 2004; 88:349–358. [PubMed: 14690523]
40. Gong R, Rifai A, Dworkin LD. Anti-inflammatory effect of hepatocyte growth factor in chronic kidney disease: targeting the inflamed vascular endothelium. J Am Soc Nephrol. 2006; 17:2464–2473. [PubMed: 16885407]
41. Zhuang S, Kinsey GR, Yan Y, et al. Extracellular signal-regulated kinase activation mediates mitochondrial dysfunction and necrosis induced by hydrogen peroxide in renal proximal tubular cells. J Pharmacol Exp Ther. 2008; 325:732–740. [PubMed: 18339970]
42. Stoyanovsky DA, Vlasova II, Belikova NA, et al. Activation of NO donors in mitochondria: peroxidase metabolism of (2-hydroxyamino-vinyl)-triphenyl-phosphonium by cytochrome c releases NO and protects cells against apoptosis. FEBS Lett. 2008; 582:725–728. [PubMed: 18258194]
43. Nieminen AL, Saylor AK, Tesfai SA, et al. Contribution of the mitochondrial permeability transition to lethal injury after exposure of hepatocytes to t-butylhydroperoxide. Biochem J. 1995; 307(Pt 1):99–106. [PubMed: 7718000]

44. Chen S, Ge Y, Si J, et al. Candesartan suppresses chronic renal inflammation by a novel antioxidant action independent of AT1R blockade. Kidney Int. 2008; 74:1128–1138. [PubMed: 18650791]

45. Ohori K, Miura T, Tanno M, et al. Ser9 phosphorylation of mitochondrial GSK-3beta is a primary mechanism of cardiomyocyte protection by erythropoietin against oxidant-induced apoptosis. Am J Physiol Heart Circ Physiol. 2008; 295:H2079–2086. [PubMed: 18805899]

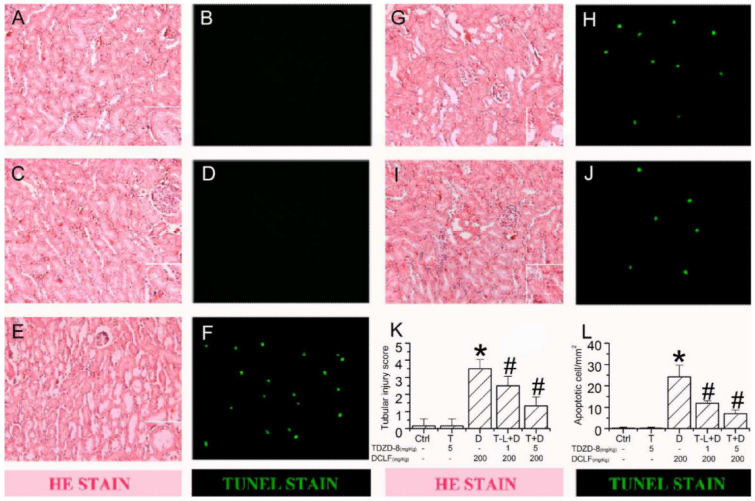

Figure 1. GSK3β inhibition protects mice from DCLF-induced renal tubular injury and cell apoptosis *in vivo*

Representative micrographs of hematoxylin and eosin (HE) staining (A, C, E, G, I) and TUNEL staining (B, D, F, H, J) of kidney specimens. A, B: Group Ctrl, control (vehicle treated); C, D: Group T, TDZD-8 (5 mg/kg); E, F: Group D, DCLF (200 mg/Kg); G, H: Group T-L+D, low dose TDZD-8 (1 mg/Kg)+DCLF (200 mg/Kg); I, J: Group T+D, TDZD-8 (5 mg/Kg)+DCLF (200 mg/Kg). K, L: Quantitative analysis of tubular injury and TUNEL-labeled cells among the groups. The results are expressed as the mean ± SD (n=6). **P*<0.05, versus Group Ctrl; #*P*<0.05, versus Group D. DCLF elicited injury to both proximal and distal tubular cells. TUNEL-labeled nuclei were revealed as bright spots in the renal cortex in kidneys from DCLF-treated mice. TDZD-8 significantly attenuated both tubular necrosis and apoptosis in mouse kidneys.

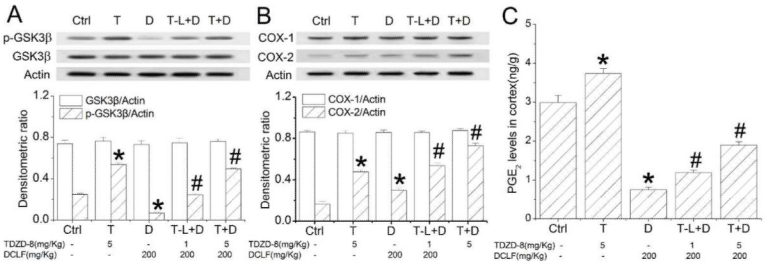

Figure 2. Effects of TDZD-8 on GSK3β phosphorylaion and the levels of COX-2 and PGE_2 in kidney cortices of DCLF-treated mice

A: Western blot analysis of GSK3β and p-GSK3β in cortical homogenate. B: Western blot analysis of COX-1 and COX-2 in cortical homogenate. C: Analysis of cortical PGE_2 in cortical homogenate. Group Ctrl, control (vehicle treated); Group T, TDZD-8 (5 mg/kg); Group D, DCLF (200 mg/Kg); Group T-L+D, TDZD-8 (1 mg/Kg)+DCLF (200 mg/Kg); Group T+D, TDZD-8 (5 mg/Kg)+DCLF (200 mg/Kg). **P*<0.05, versus Group Ctrl; #*P*<0.05, versus Group D. COX-1 expression was maintained and COX-2 expression was increased following treatment with DCLF. GSK3β inhibition led to a further increase in COX-2 expression in the renal cortices of DCLF-treated mice. Accordingly, PGE_2 synthesis was increased in TDZD-8 treated mice.

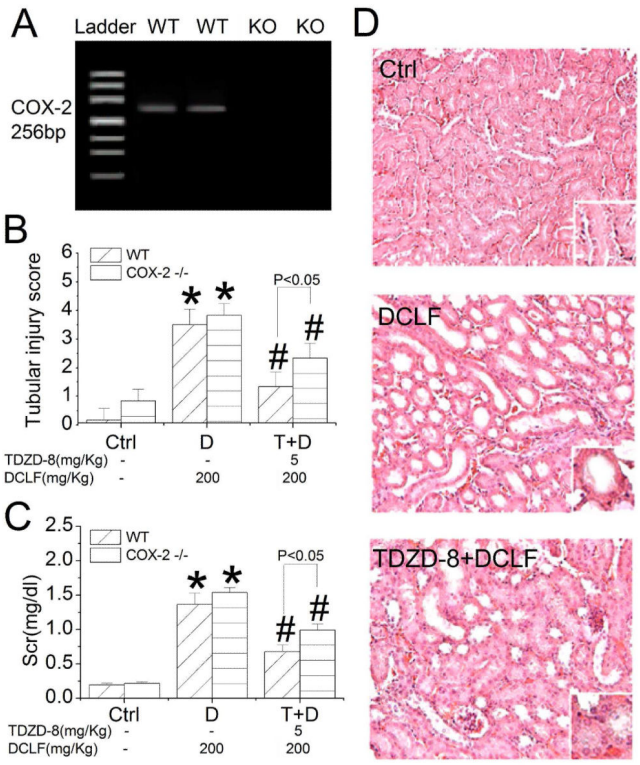

Figure 3. GSK3β inhibition protects COX-2 −/− mice from DCLF-induced renal tubular injury

A: mRNA expression of COX-2 detected by RT-PCR in the kidneys of wild-type (WT) and COX-2 knockout (KO) mice. B: Tubular injury score of WT and COX-2 KO mice treated with DCLF (200 mg/Kg) and/or TDZD-8 (5 mg/Kg). C: Serum creatinine (Scr) of WT and COX-2 KO mice treated with DCLF (200 mg/Kg) and/or TDZD-8 (5 mg/Kg). D: Representative micrographs of hematoxylin and eosin staining of kidney specimens from COX-2 KO mice treated with DCLF (200 mg/Kg) and/or TDZD-8 (5 mg/Kg). Ctrl, control (vehicle treated). **P*<0.05, versus control; #*P*<0.05, versus DCLF-treated mice. DCLF produced injury to both proximal and distal tubular cells. This kidney protective effect of TDZD-8 was blunted but still largely preserved in COX-2 null mice.

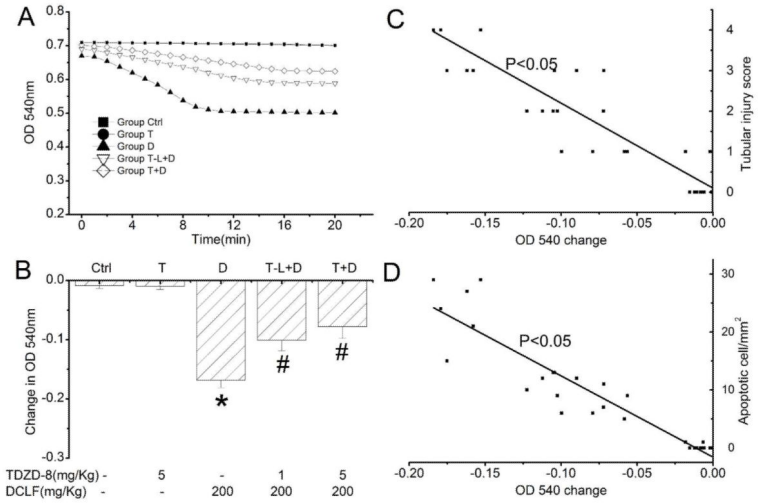

Figure 4. Effects of GSK3β inhibition on the induction of the MPT by DCLF in mouse kidneys

A: Mitochondrial swelling was spectrophotometrically monitored at 540 nm following induction with 20 M $CaCl_2$ for 20 min. B: Change in absorbance at OD540 nm after 20 min. C: Correlation between decreased absorbance at 540 nm and the renal tubular injury score. D: Correlation between decreased absorbance at 540 nm and the number of apoptotic cells in renal tissues. Group Ctrl, control (vehicle treated); Group T, TDZD-8 (5 mg/kg); Group D, DCLF (200 mg/Kg); Group T-L+D, TDZD-8 (1 mg/Kg)+DCLF (200 mg/Kg); Group T +D, TDZD-8 (5 mg/Kg)+DCLF (200 mg/Kg). **P*<0.05 versus Group Ctrl; #*P*<0.05 versus Group D. The decrease in absorbance at 540 nm was negatively correlated with the number of apoptotic cells and the renal tubular injury scores in mouse kidneys. Mitochondria that were isolated from kidneys treated with DCLF displayed an increased rate of mitochondrial swelling and a greater decrease in absorbance at 540 nm versus the controls, while TDZD-8 treatment ameliorated this process in a dose-dependent fashion.

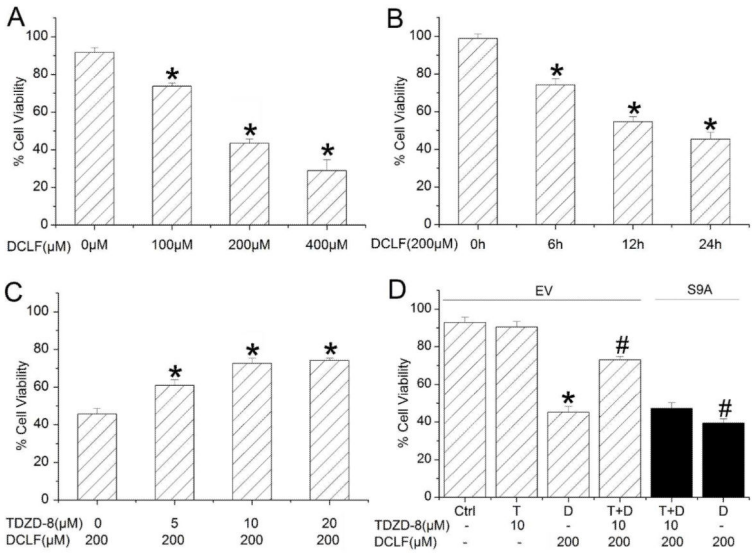

Figure 5. Effects of GSK3β inhibition on the viability of renal tubular epithelial cells injured with DCLF

A: Viability of TKPT cells following treatment with different doses of DCLF (DCLF, 0, 100, 200, 400 μM) for 24 h. **P*<0.05 versus normal controls; n=6. B: Survival rate of TKPT cells after treatment with 200 μM DCLF for different times. **P*<0.05 versus the beginning; n=6. C: Survival rate of TKPT cells pretreated with different doses of TDZD-8 (0, 5, 10, 20 μM) and then treated with 200 μM DCLF for 24 h. **P*<0.05 versus DCLF-treated cells; n=6. D: Survival rate of TKPT cells expressing either empty vector or S9A-GSK3β after treatment with 200 μM DCLF, 10 μM TDZD-8 or combined treatment. EV, empty vector transfected TKPT cells; S9A, S9A-GSK3β transfected TKPT cells; Ctrl, control; T, TDZD-8 10 μM; D, DCLF 200 μM. **P*<0.05 versus control cells; #*P*<0.05 versus the value of empty vector-transfected cells treated with DCLF. Treatment with DCLF markedly decreased cell viability in a time- and dose-dependent manner, while treatment with TDZD-8 improved survival rates (*P*<0.05). In contrast, the supportive effect of TDZD-8 was blunted in cells transfected with vectors carrying S9A-GSK3β, a mutant of GSK3β that is unable to be phosphorylated at serine 9.

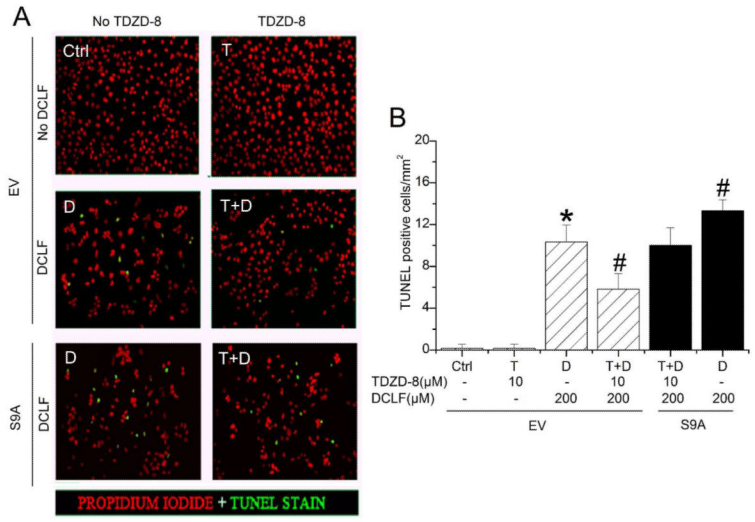

Figure 6. Effect of GSK3β inhibition on the apoptosis of TKPT cells treated with DCLF

A: TKPT cells were treated as indicated, fixed and exposed to TdT-mediated dUTP nick-end labeling (TUNEL) to assess apoptosis. B: Quantitative assessment of cell apoptosis. Cells in a ×200 field were manually counted in 10 fields per slide, with three replicates. EV, empty vector transfected TKPT cells; S9A, S9A-GSK3β atransfected TKPT cells; Ctrl, control; T, TDZD-8 10 M; D, DCLF 200 M. **P*<0.05 versus control cells; #*P*<0.05 versus empty vector transfected cells treated with DCLF; n=6. There was a significant increase in the number of apoptotic cells following exposure to DCLF versus controls after 24 h (*P*<0.05). The number of apoptotic cells was decreased to approximately five per field in cultures pre-treated with TDZD-8, while the anti-apoptotic effect of TDZD-8 was attenuated in cells expressing S9A-GSK3β.

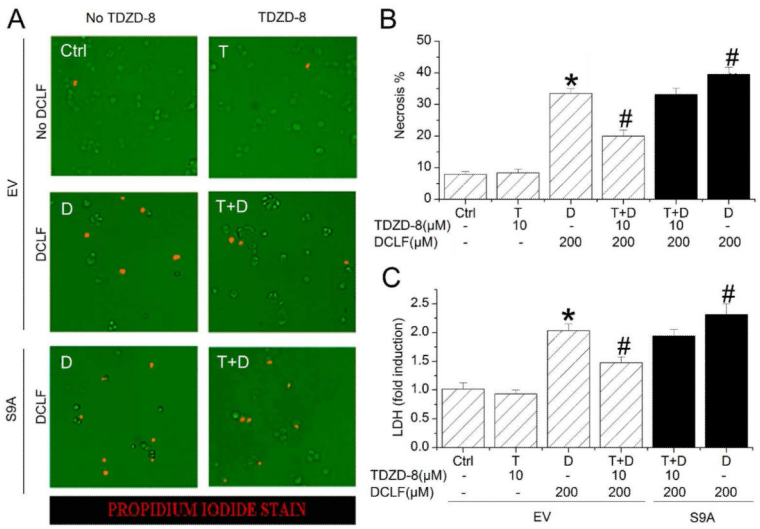

Figure 7. Effects of GSK3β inhibition on the necrosis of TKPT cells exposed to DCLF

A: Necrotic cell death was assessed using the propidium iodide exclusion assay in live cells. B: Quantitative assessment of cell necrosis by propidium iodide exclusion assay. Cells in a ×200 field were manually counted in 10 fields per slide, with three replicates. C: Necrotic cell death was assessed by lactate dehydrogenase (LDH) assay of the conditioned medium. EV, empty vector transfected TKPT cells; S9A, S9A-GSK3β transfected TKPT cells; Ctrl, control; T, TDZD-8 10 M; D, DCLF 200 M. **P*<0.05 versus control cells; #*P*<0.05 versus empty vector transfected cells treated with DCLF; n=6. There was a significant increase in the number of necrotic cells and in LDH release in cultures exposed to DCLF versus controls after 24 h (*P*<0.05). TDZD-8 treatment decreased the number of necrotic cells and the LDH level, while the effects of TDZD-8 were attenuated in cells transfected with S9A-GSK3β.

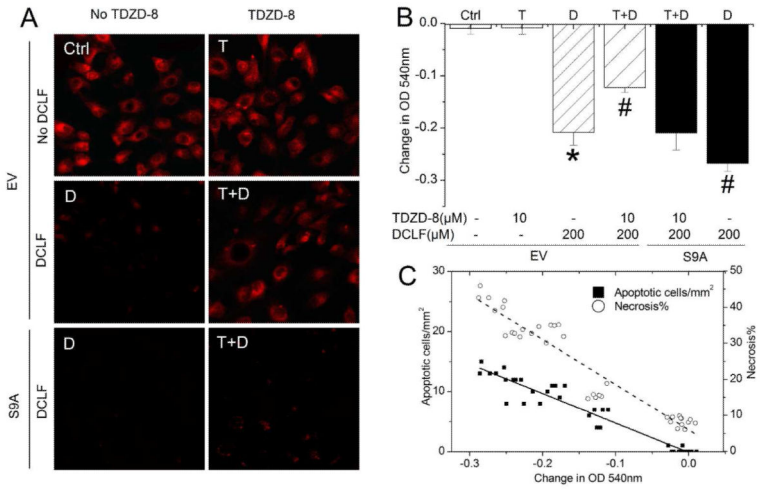

Figure 8. Effects of GSK3β inhibition on MPT in TKPT cells exposed to DCLF

A: TMRM was used to detect the onset of the MPT by fluorescence microscopy. B: Mitochondrial swelling was spectrophotometrically monitored at 540 nm in mitochondria that had been induced with 20 M $CaCl_2$ for 20 min. EV, empty vector transfected TKPT cells; S9A, S9A-GSK3β transfected TKPT cells; Ctrl, control; T, TDZD-8 10 M; D, DCLF 200 M. **P*<0.05 versus control cells; #*P*<0.05 versus empty vector transfected cells treated with DCLF; n=6. C: Correlation between the decrease in absorbance at 540 nm and the number of apoptotic or necrotic cells. Mitochondria that were isolated from cells treated with DCLF displayed quenching of TMRM and decreased absorbance at 540 nm compared to mitochondria from control cells. The extent of the decrease in absorbance at 540 nm was correlated with both the number of apoptotic and necrotic cells. Pretreatment with TDZD-8 inhibited the quenching of TMRM and restored the capacity of mitochondria that had been subjected to DCLF to accumulate calcium. All of these effects were blunted in cells expressing S9A-GSK3β.

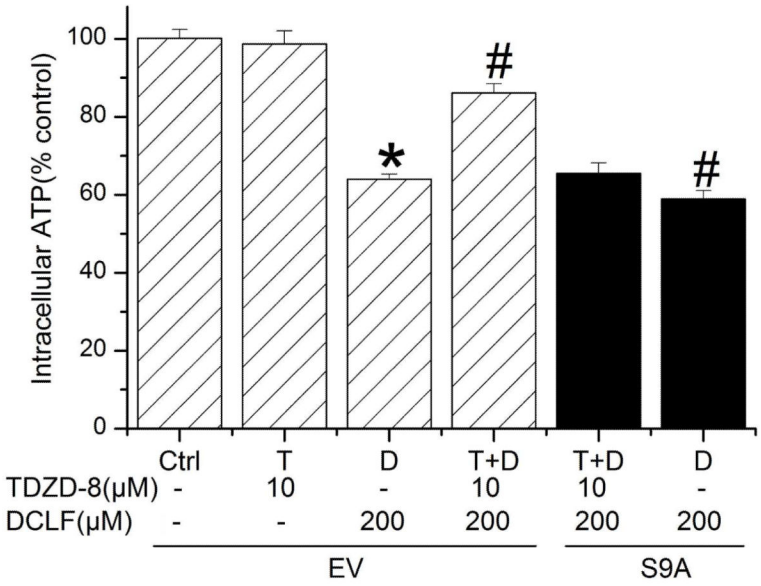

Figure 9. Effect of GSK3β inhibition on intracellular ATP content in TKPT cells treated with DCLF

ATP concentration was measured using the luciferase method. EV, empty vector transfected cells; S9A, S9A-GSK3β transfected TKPT cells; Ctrl, control; T, TDZD-8 10 M; D, DCLF 200 M. **P*<0.05 versus control cells; #*P*<0.05 versus empty vector transfected cells treated with DCLF; n=6. Treatment with DCLF significantly decreased ATP production. Treatment with TDZD-8 increased intracellular ATP, and the effect was blunted in cells transfected with S9A-GSK3β.

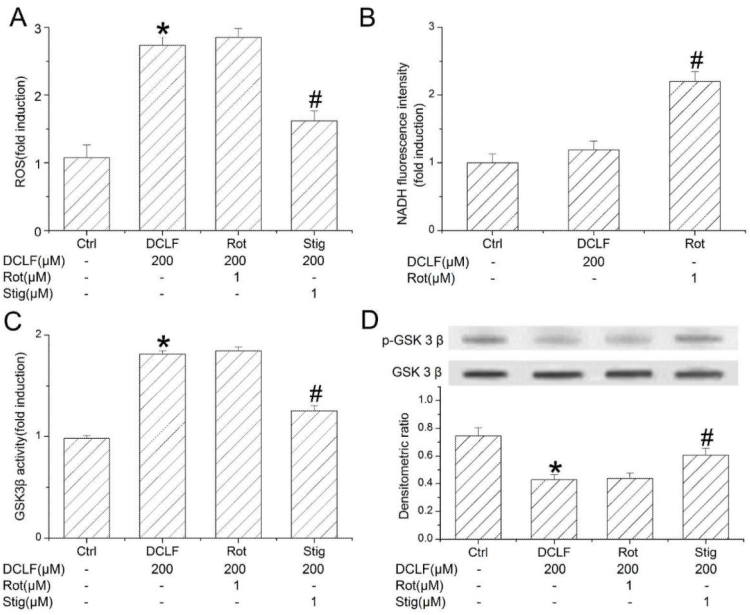

Figure 10. Effect of DCLF on redox-sensitive GSK3β in TKPT cells

TKPT cells were treated with 200 M DCLF or pretreated with 1 M rotenone (Rot) or 1 M stigmatellin (Stig). A: ROS formation was evaluated by the oxidation of DCFH-DA to the fluorescent DCF in TKPT cells. B: NADH dehydrogenase activity in mitochondrial extracts was compared by the fluorescence of NADH at the fifth minute after the start of assay. C: GSK3β activity was assayed by measuring the incorporation of ^{32}P into the substrate. D: Western blot analysis of GSK3β and p-Ser9-GSK3β expression in cells. **P*<0.05 versus control cells; #*P*<0.05 versus cells treated with DCLF; n=6. DCLF treatment induced ROS production and GSK3β activation in TKPT cells but did not affect NADH dehydrogenase activity. Stigmatellin significantly suppressed ROS production and GSK3β activation in DCLF-treated TKPT cells, whereas rotenone had no effect.

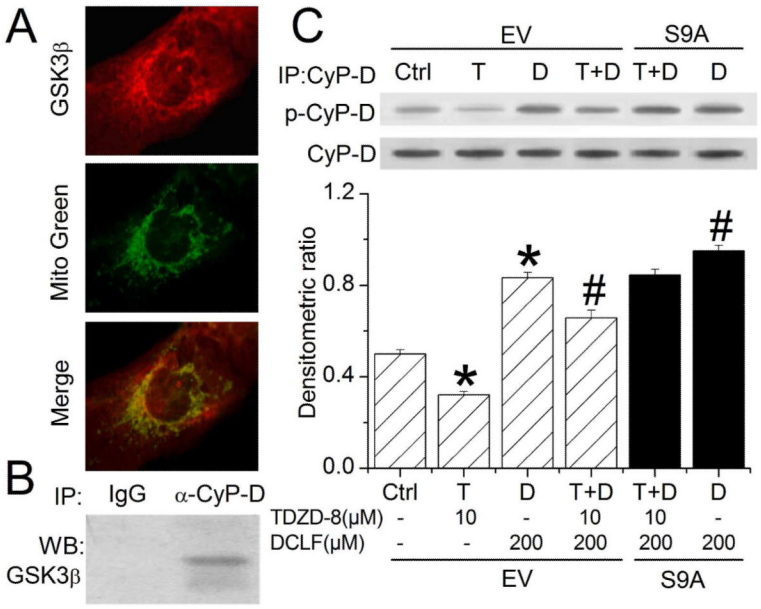

Figure 11. GSK3β colocalizes with cyclophilin D, a component of the MPT pore complex, and regulates its activation

A: Representative images of the co-localization of GSK3β with mitochondria in TKPT cells. B: TKPT cell mitochondria were purified, immunoprecipitated with anti-cyclophilin D antibody, and immunoblotted with anti-GSK3β antibody. C: TKPT cell mitochondria were separated, immunoprecipitated with anti-cyclophilin D antibody, and immunoblotted with anti-phosphorylated-serine antibody. EV, empty vector transfected cells; S9A, S9A-GSK3β transfected TKPT cells; Ctrl, control; T, TDZD-8 10 M; D, DCLF 200 M. **P*<0.05 versus control cells; #*P*<0.05 versus empty vector transfected cells treated with DCLF; n=6. GSK3β co-localized with cyclophilin D in the mitochondria. DCLF treatment significantly increased the phosphorylation of cyclophilin D. Inhibition of GSK3β by TDZD-8 suppressed the phosphorylation of cyclophilin D, whereas this effect was diminished in cells transfected with S9A-GSK3β.

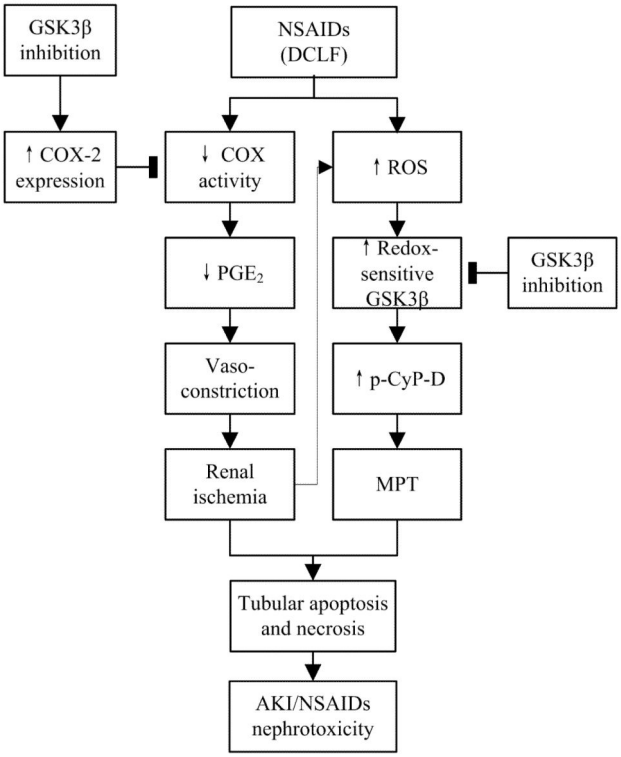

Figure 12. GSK3β inhibition prevents NSAID-induced acute kidney injury by dual mechanisms

Over-inhibition of prostaglandin synthesis by NSAIDs leads to renal ischemia, a decline in glomerular hydraulic pressure and acute renal failure. DCLF is also able to injure renal tubular epithelial cells directly by triggering ROS production, enhancing the activity of redox-sensitive GSK3β, and thereby promoting cyclophilin D phosphorylation and the ensuing MPT pore opening. GSK3β inhibition prevents NSAID-induced acute kidney injury via both the induction of cortical cyclooxygenase-2 and the inhibition of the MPT.

Table 1

Changes of body weight, kidney weight and serum creatinine levels after different treatments

Group	Ctrl	T	D	T-L+D	T+D
Base Weight(g)	19.1±1.0	19.8±0.8	19.8±0.9	19.6±0.7	19.3±0.6
Weight change(g)	0.01±0.16	−0.07±0.09	−1.44±0.20*	−0.85±0.10#	−0.55±0.12#
Kidney weight(mg)	127.0±3.6	124.6±3.3	176.4±9.9*	158.7±6.8#	148.0±3.5#
sCr(mg/dl)	0.19±0.03	0.21±0.02	1.36±0.16*	0.98±0.20#	0.67±0.10#

Notes: sCr, serum creatinine. Group Ctrl: control mice treated with vehicle; Group T: TDZD-8 (5mg/kg) treated mice; Group D: DCLF (200mg/Kg) injured mice; Group T-L+D: low dose TDZD-8 (1mg/Kg) +DCLF (200mg/Kg) treated mice; Group T+D: TDZD-8 (5mg/Kg) + DCLF (200mg/Kg) treated mice.

*P<0.05, versus Group Ctrl

#P<0.05, versus Group D.